AADE-03-NTCE-58

Advanced Laminar Flow Oil/Water Separation Technology

Naji Nassif, Gnesys, Inc. and William Ney Hansard, Environmental Management Services, Inc.

Copyright 2003 AADE Technical Conference

This paper was prepared for presentation at the AADE 2003 National Technology Conference "Practical Solutions for Drilling Challenges", held at the Radisson Astrodome Houston, Texas, April 1 - 3, 2003 in Houston, Texas. This conference was hosted by the Houston Chapter of the American Association of Drilling Engineers. The information presented in this paper does not reflect any position, claim or endorsement made or implied by the American Association of Drilling Engineers, their officers or members. Questions concerning the content of this paper should be directed to the individuals listed as author/s of this work.

Abstract

In oil/water separation, it is customary to refer to Stokes' Law for calculating bubble rise velocity, and estimating residence time in order to size an oil/water separator. This approach does not adequately take into account other physical or chemical factors, and generally works adequately only when a significant scale-up factor is used.

A completely new design approach to oil/water separation has been developed based on careful observations of oil/water separation phenomena.

In pipe flow experiments, it was observed that in addition to the drag forces, radial lift forces and particle rotation are caused by the velocity gradient across the pipe. The same phenomenon occurs in laminar flow between two flat plates. The velocity gradient between the plates causes rotation of the particle (or oil bubble,) which in turn induces lateral lift. The bubble is pushed towards the wall region where velocities approach zero. As more oil bubbles agglomerate near the wall, chances for coalescence are increased.

These dynamics were applied in the design of a new type of oil water separator. results obtained from a variety of applications showed efficiencies in excess of 99% under severe conditions.

An innovative approach to oil/water separation is now available. It is based on innovative concepts of the physical interactions of oil and water in controlled laminar flow conditions.

Introduction

Traditionally, the rate of rise of an oil particle in an oil water separator is obtained by applying Stokes' Law to a measured or assumed particle diameter. This generally accepted method fails to provide good correlation with data for the following reasons: estimated particle size versus actual particle size distribution, the presence of particulate impurities, or other chemicals in the water or influent oil concentrations in excess of that used for design. Stokes' Law is obtained by simplifying the three-dimensional Navier-Stokes equation,

$$\rho_c\left[\underbrace{\frac{\partial\tilde{v}}{\partial t}}_{\substack{Accum.\\ Term}}+\underbrace{\tilde{v}\cdot\nabla\tilde{v}}_{\substack{Inertia\\ Forces}}\right]=\underbrace{-\nabla p}_{\substack{Pressure\\ Forces}}+\underbrace{\mu_c\nabla^2\tilde{v}}_{\substack{Viscous\\ Forces}}+\underbrace{\rho_c\tilde{g}}_{\substack{Gravity\\ Forces}} \qquad (1)$$

for the conditions of steady Newtonian creeping flow about a solid non-rotating fixed sphere with zero slip at its surface[1]. The restrictions on the problem leave us with the following boundary conditions: $v_r(R) = 0$, $v_\theta(R) = 0$ and $v_\phi(R) = 0$, $v_r(\infty) = v_\infty$, which, when applied to equation (1) above yields, after eliminating the accumulation and inertia terms, the one-directional total force, F, that the fluid exerts on the sphere

$$F=\underbrace{\tfrac{1}{6}\pi D^3\rho_c g}_{\substack{Buoyant\\ Force}}+\underbrace{\pi\mu_c D v_\infty}_{\substack{Form\\ Drag}}+\underbrace{2\pi\mu_c D v_\infty}_{\substack{Friction\\ Drag}} \qquad (2)$$

Combining the form and friction drag terms,

$$F=\underbrace{\tfrac{1}{6}\pi D^3\rho_c g}_{\substack{Buoyant\\ Force}}+\underbrace{3\pi\mu_c D v_\infty}_{\substack{\left(\begin{smallmatrix}Kinetic\\ Force\end{smallmatrix}\right)=\left(\begin{smallmatrix}Stokes'\\ Law\end{smallmatrix}\right)}} \qquad (3)$$

Assuming that the sphere is held in place due to its own weight, $F = m_s g = \rho_s V_s g$ and substituting in equation (3) by setting the terminal velocity, $v_t = v_\infty$

$$v_t=\frac{1}{18}\frac{gD^2}{\mu_c}\left(\rho_s-\rho_c\right) \qquad (4)$$

The kinetic force (Stokes' law term) is also defined as[1]

$$F_k=\frac{\pi D^2}{4}\left(\tfrac{1}{2}\rho_c v_\infty^2\right)f \qquad (5)$$

Where combining equations 4 and 5 yields

$$f=\frac{24}{\mathrm{Re}} \qquad (6)$$

Figure 1 compares equation 6, the drag coefficient obtained from Stokes' Law to the actual drag curve for a sphere obtained from wind and water tunnel measurements[2]. The Stokes' Law drag coefficient correlates well with actual drag on a solid sphere for a Reynolds number of up to 0.1[1]. At a Reynolds number of 1, Stokes' Law underpredicts the drag over a sphere by about 10%. At a Reynolds number of 10, the drag is underpredicted by a factor of 4.5. Both Stokes' Law and the actual drag curve apply to solid non-rotating spheres either moving at a constant velocity and in a straight line or subjected to a constant velocity infinite fluid.

We are however trying to separate two liquid media – a continuous phase and a dispersed phase. Interfacial tension becomes predominant over gravity as the bubbles get smaller, creating an emulsion. Unlike a solid sphere, a liquid sphere can experience internal circulation implying that the velocity components at the surface are no longer necessarily zero and slippage occurs increasing the rate of rise of the bubble. A modification of Stokes' analysis to account for circulation and surface effects for a liquid sphere moving in a quiescent fluid is given as[3]

$$\frac{v_{tc}}{v_t} = \frac{3\mu_d + 3\mu_c + \gamma}{3\mu_d + 2\mu_c + \gamma} \qquad (7)$$

In the absence of surface active agents, γ = 0 and the terminal velocity of a liquid bubble is greater than that predicted by Stokes' Law. Equation 7 was found valid for Reynolds numbers less than 4. The drag increased between 4 and 10 due to the presence of a ring vortex. Between 10 and 40, the drag followed the solid sphere line. Between 40 and 45 the drag increased above the solid sphere line. Vortex break-up began at 45 and vortex shedding was observed past 100. The bubble rise path shifted from a straight line to a helical path at 300[4].

Experiments were performed in a vertical cylindrical tube on an initially uniform dilute suspension of rigid spheres in an equal-density fluid at low Reynolds numbers. The tube diameter was 11.2 mm and the spheres varied from 0.32 to 1.71 mm. In addition to the drag forces, radial lift forces and particle rotation caused by the velocity gradient were observed. The particles were observed to move away from the centerline and the wall to a radial position approximately 0.6 the tube radius[5]. The radial particle migration away from the centerline could be attributed to the Magnus effect[3]. The migration away from the wall could be attributed to self-lubrication in pipelines[6] as the mixture of continuous phase and solid spheres has a higher average viscosity than the continuous phase.

Theory Behind Separator Design

The same phenomenon observed in laminar flow in a pipe could be anticipated for laminar flow between two flat plates with planar instead of radial symmetry. The velocity gradient induced rotation and lateral lift tend to push the particles towards the walls, where low velocities are present. Hence, residence time is increased in the channel allowing more time for separation. As more bubbles agglomerate near the wall chances for coalescence are increased. Figure 2 is a schematic of the induced spin in laminar flow.

If the plates were horizontal or inclined, the lateral lift could be aided or opposed by gravity and buoyancy depending on where the bubble lies with respect to the plane of symmetry. However, if the channel plates were vertical then lateral lift, which is perpendicular to the flow direction, would also be perpendicular to gravity and buoyancy forces. All three velocity components would then be perpendicular to each other and would not interfere with each other. Hence, an entrained particle with a specific gravity less than that of the carrying liquid would be spun towards the wall as it tries to rise. If the vertical plates are spaced to have a small width, W, to height, H, aspect ratio, then, for a constant volumetric flow rate Q, the initial average velocity in the channel can be expressed as,

$$v = \frac{Q}{HW} \qquad (8)$$

The initial residence time is defined as

$$\tau = \frac{L}{v} \qquad (9)$$

As oil builds up in the channel, the working height of the channel becomes

$$H' = \alpha H \qquad (10)$$

where α is between 0 and 1. The velocity becomes

$$v' = \frac{Q}{H'W} = \frac{Q}{\alpha HW} \qquad (11)$$

Combining equation 8 with 11

$$v' = \frac{v}{\alpha} \qquad (12)$$

and the new residence time becomes

$$\tau' = \frac{L}{v'} = \frac{\alpha L}{v} = \alpha\tau \qquad (13)$$

The minimum required rise velocity for an oil particle to reach the surface prior to leaving the separator channel is

$$v = \frac{H}{\tau} \tag{14}$$

and the minimum required rise velocity for an oil particle to reach the interface after oil build-up prior to leaving the separator channel is

$$v' = \frac{H'}{\tau'} = \frac{\alpha H}{\alpha \tau} = v \tag{15}$$

Hence, despite oil build-up, the required rise velocity for an oil particle to reach the interface remains constant.

Description of Separator

Figure 3 is a top view of the separator layout. The designed vessel has a first chamber, called the mixture section, for trapping sediment and diffusing the inlet pipe velocities. A baffle which extends the entire height of the vessel and about three-fourths its width separates this chamber from the separating section. The separating section is divided into a number of channels in series laid out in a serpentine fashion such that the flow travels through this section back and forth at least five times. These channels are divided by a number of vertical plates to form parallel sub-channels having a small width to height ratio. The Reynolds number in each of the channels is reduced by the number of sub-channels. The width and height of the channels and sub-channels are optimized to maximize retention time in a given footprint, maintain laminar flow between the plates, but keep a wide enough space to prevent clogging. A pipe and an opening in the second baffle defining the separating section are located diagonally opposite from the opening in the first baffle. The opening leads to the oil (removal) section. Another purpose of this chamber is to automate oil removal. The pipe's elevation is set to allow the water to be transferred to a final chamber for discharge. Its length and diameter are designed to ensure that the air gap created by locating the outlet invert in the side wall acts as an accumulator to dampen sudden inrushes and any flow accelerations.

The lighter oil accumulates on top of the water across the first three chambers. As more oil is accumulated, the layer thickens and water is pushed out the pipe to the clean water section where it exits through the outlet. The liquid level is controlled by the outlet invert. The accumulated oil displaces the water through the pipe to the last chamber and out through the outlet. The usable cross-section in each channel diminishes and the velocity increases accordingly leading to higher Reynolds numbers. Equation 15 demonstrates that the removal efficiency of the separator is not affected by oil build-up provided laminar flow is maintained.

Field Tests of Design

A spill simulation was performed at a TVA power plant on an HS-15000 model separator. The contents of the existing concrete API type separator (3,500 gal.), water, oil and sludge, were pumped out and transferred to the HS 15000. Fire hydrant water at approximately 250 gpm was run through the separator for 1.5 hrs prior to the spill. 800 gallons of Diesel were spilled at 400 gpm in the catch basin leading to the separator inlet where the fire hydrant water was being discharged to provide proper mixing. The fire hydrant water was left running for another 75 minutes to ensure approximately one and a half volume changes within the separator. Sampling was done at 5-minute intervals for the 75 minutes and the samples were taken to an independent laboratory for analysis. Figure 4 is a graph of the results. The minimum and maximum oil and grease content were 9 and 20.8 mg/L with an average of 12.44 mg/L. The total amount of oil lost from the 800-gallon spill amounts to 0.28 gallons. The figure below is a graphical representation of the data. The input oil/water mixture is estimated at 510,000 mg/L. Two effluent samples were also taken during the 3,500-gallon liquid transfer from the old separator 15 minutes apart. The results were 24 and 42 mg/L respectively. This can be mainly attributed to the high sludge, oil and dissolved substances present in the old separator.

Another series of tests performed on the effluent of a vegetable oil plant where the average inlet pH was 3.9 yielded efficiencies between 72% and 95%. Other parameters such as TSS and COD also showed significant improvement. More importantly, concentration spikes in the input were dampened at the output, a feature most beneficial for post-treatment devices. Figure 5 depicts inlet and outlet concentrations of fats, oils and greases versus time. The residence time was subtracted from the outlet sampling time to better match it with its corresponding input. Additional tests were performed at varying pH levels.

An HS-1200 (1,200 gallon volume) rectangular separator was installed at a major aluminum die-casting facility to treat the entire plant's waste stream. The plant wastewater was contaminated with heavy greases, a variety of lubricating oils, glycol, die-spray, testing and cutting oils and fluids from machine shops as well as machining and deburring chips. The HS-1200 separator received a flow ranging from 10,000 to 16,000 GPD. The estimated efficiencies listed in table 1, along with the separator spike-dampening characteristics, have helped improve the facility's treatment plant performance, chemical usage and treatment plant maintenance record. It should be noted that the oil removal is automated in this application and that the oil pump is activated when the oil layer exceeds

approximately 30% of the useful liquid column.

Conclusions

In this paper, the limitations of Stokes' Law were discussed. In gravity separators, neither the continuous phase nor the particles are fixed and their interaction is seldom in the "creeping flow" regime, both factors fundamental to oil/water separator design using Stoke's Law. Smaller liquid bubbles, which remain spherical, are subjected to slippage and more importantly interfacial tension.

In contrast, the separator design discussed in this paper relies on the establishment of a two-dimensional laminar velocity profile in the continuous phase to impart spin on the particles dispersed within.

A simple theoretical derivation showed that, in the same flow regime, the efficiency of the vessel should not be affected by the accumulation of oil in the separator. The vessel installed at the aluminum die-casting facility, with its 30% oil layer thickness helps in proving this assumption.

An innovative approach to oil/water separation is now available. It is based on innovative concepts of the physical interactions of oil and water in controlled laminar flow conditions.

Nomenclature

D = *diameter of sphere*
F = *total force exerted by fluid on sphere*
F_k = *kinetic force acting on sphere*
f = *drag coefficient*
$\tilde{g}$ = *gravitational vector*
g = *gravitational constant*
H = *initial height of separator flow channel*
H' = *height of separator flow channel after oil build-up*
L = *length of separator channel*
m_s = *mass of sphere*
Q = *volumetric flow rate in separator flow channel*
p = *pressure force*
R = *radius of solid sphere*
r, θ, ϕ = *spherical coordinate system*
t = *time*
V_s = *volume of sphere*
v = *initial average velocity of fluid in separator channel*
v' = *average velocity of fluid in separator channel after oil build up*
$\tilde{v}$ = *flow velocity vector*
v_r, v_θ, v_ϕ = *flow velocity components in spherical coordinates*
v_t = *terminal velocity of solid sphere*
v_{tc} = *corrected terminal velocity of liquid sphere*
v_∞ = *velocity of fluid in pipe away from sphere*
W = *width of separator flow channel*
α = *ratio of H' to H.*
γ = *retardation coefficient of surface active agents*
ρ_c = *density of continuous fluid*
ρ_d = *density of liquid sphere*
ρ_s = *density of solid sphere*
μ_c = *dynamic viscosity of continuous fluid*
μ_d = *dynamic viscosity of liquid sphere*
τ = *initial residence time in separator flow channel*
τ' = *residence time in separator flow channel after oil build-up*
v = *initial minimum required oil bubble rise velocity in separator channel*
v' = *minimum required oil bubble rise velocity in separator channel after oil build up*
∇ = *del operator*
∇^2 = *Laplacian operator*

References

1. Bird, R., Stewart, W., Lightfoot, E., "Transport Phenomena," John Wiley & Sons, 1960.
2. Janna, W., "Introduction to Fluid Mechanics," PWS Publishers, 2nd Edition, 1987.
3. Brodkey, R., "The Phenomena of Fluid Motions," Dover, 1967.
4. Satapathy, R., Smith, W., "The Motion of Single Immiscible Drops Through a Liquid," J. of Fluid Mechanics, 1961, **10**, 561-570.
5. Segré, G., Silberberg, A., "Behaviour of Macroscopic Rigid Spheres in Poiseuille Flow Part 2. Experimental Results and Interpretation," J. of Fluid Mech., 1962, **14**, 115-157.
6. Joseph, D., Renardy, Y., "Fundamentals of Two-Fluid Dynamics. Part I: Mathematical Theory and Applications," Springer-Verlag, 1993.

Figures

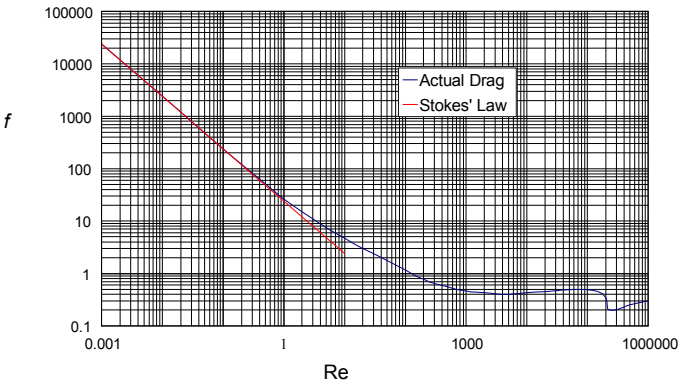

Figure 1 Comparison of Actual Drag and Stokes' Law Drag versus Reynolds Number

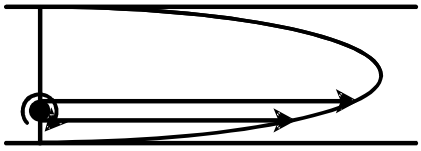

Figure 2 Induced Spin Caused by Laminar Velocity Profile.

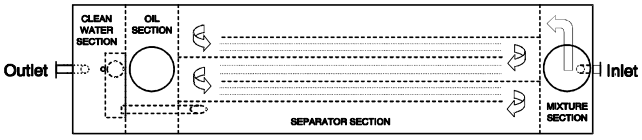

Figure 3 Top view of a separator designed to take advantage of bubble spin.

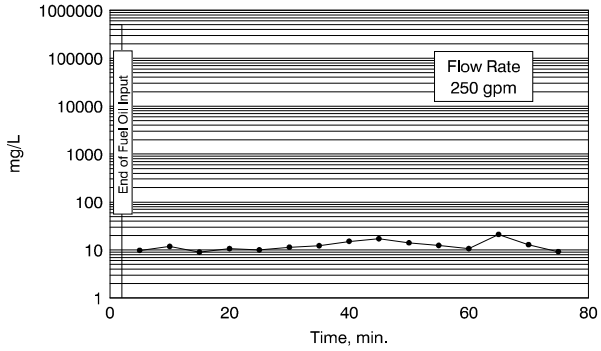

Figure 4 Spill simulation at an actual installation. During the spill, the flow rate was 650 gpm.

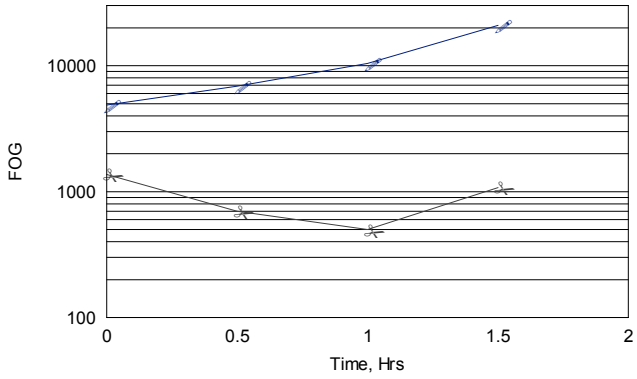

Figure 5 Comparison of inlet and outlet samples from an HS-1290 separator subjected to a slipstream from a vegetable oil plant.

	BOD	COD	O&G	TSS	pH
	mg/l	mg/l	mg/l	mg/l	Units
Estimated Raw Influent	20k	200k	120k	100k	6.5-9.0
Effluent Composite Sample	1.3k	25k	0.85k	1.2k	8.5
% Efficiency	94	88	>99	99	N/A

Table 1 Comparison of inlet and outlet from an HS-1200 at an aluminum die-casting facility.